Journal of Magnetic Resonance 201 (2009) 205–211

Contents lists available at ScienceDirect

Journal of Magnetic Resonance

journal homepage: www.elsevier.com/locate/jmr

Deriving time-dependent diffusion and relaxation rate in porous systems using eigenfunctions of the Laplace operator

Matias Nordin [a,*], Martin Nilsson Jacobi [b], Magnus Nydén [a]

[a] Applied Surface Chemistry, Department of Chemical and Biological Engineering, Chalmers University of Technology, 412 96 Gothenburg, Sweden
[b] Complex Systems Group, Department of Energy and Environment, Chalmers University of Technology, 412 96 Gothenburg, Sweden

ARTICLE INFO

Article history:
Received 8 April 2009
Revised 4 September 2009
Available online 11 September 2009

Keywords:
Restricted diffusion
Padé approximation
Porous system
Padé length
Tortuosity
Void space
Discrete Laplacian
Relaxation rate
Spectral gap

ABSTRACT

Porous systems are investigated using eigendecomposition of the Laplace matrix. Three parameters; tortuosity, surface-to-pore volume ratio and relaxation rate are derived from the eigenvalue spectrum of the Laplace matrix and connected to the parameters in the Padé approximation, an expression often used to describe the time-dependent diffusion coefficient in porous systems. The Padé length is identified for systems with large pore to connector volume ratio. The results are compared with simulations.

1. Introduction

A porous material consists of pores and connectors between the pores. Diffusion of gas or liquid (henceforth referred to as particles) in porous systems is often described with a time dependent diffusion coefficient $D(t)$, defined as

$$D(t) = \frac{\left\langle (\mathbf{r}_0 - \mathbf{r}(t))^2 \right\rangle}{2nt}, \tag{1}$$

in n dimensions. In a material consisting of pores with narrow connectors (narrow when compared to the typical length scale of the pores), the behavior of $D(t)$ can be divided into three time regions. At very short observation times, $D(t)$ is dominated by the unrestricted diffusion constant D_0 which is directly obtained from the width of the Gaussian diffusion propagator typical for unrestricted diffusive transport. For intermediate observation times, the time-dependent diffusion coefficient $D(t)$ is lower than D_0 as the particles have started to collide with the obstructing walls. Due to the influence from the local pore and connector geometry, the diffusion propagator displays a complicated non-Gaussian behavior in this region. Finally, in the long time limit the particles move in a pore-to-pore mode and the transport can effectively be described as a jump process between pores making the diffusion propagator again approximately Gaussian. In this region $D(t)$, converges to the stationary value D_∞. The pore-to-pore behavior has been studied previously, see for example [1–3]. The physical interpretation is that the particles resume a diffusive behavior on a scale much larger than the size of the pores. On this scale, the diffusion is said to be dominated by the diffusive *tortuosity* τ, defined as [4]

$$\frac{1}{\tau} = \lim_{t\to\infty} \frac{D(t)}{D_0}. \tag{2}$$

Since it is difficult to treat the intermediate non-Gaussian regime, the term *relaxation rate* is often used to describe the rate at which $D(t)$ relaxes to the long time stationary value D_∞. However a detailed analysis of the relaxation rate in porous materials is still lacking [5].

Latour et al. have proposed an interpolation between the short time region and the long time region, using a two point Padé approximation [6]. This approximation connects the short and long time region via a phenomenological relaxation parameter θ. The Padé approximation is to our knowledge not verified theoretically, but is used in simulations [7,8] and in experiments [9–13] as a good approximation of $D(t)$ although it is not always correct [13]. The approximation is written as

$$\frac{D(t)}{D_0} = 1 - \left(1 - \frac{1}{\tau}\right) \times \frac{A\sqrt{t} + (1 - 1/\tau)(t/\theta)}{(1 - 1/\tau) + A\sqrt{t} + (1 - 1/\tau)(t/\theta)}, \tag{3}$$

* Corresponding author. Fax: +46 30060062.
E-mail address: matias@chalmers.se (M. Nordin).

1090-7807/$ - see front matter © 2009 Elsevier Inc. All rights reserved.
doi:10.1016/j.jmr.2009.09.010

where A is a constant (to be explained below). Theoretical work by Mitra et al. [14,15] have shown that the initial slope of $D(t)$ in porous systems can be characterized by the relation

$$D(t)/D_0 = 1 - \frac{4\sqrt{D_0 t}}{3n\sqrt{\pi}}(S/V_p) + O(D_0 t)t \ll 1, \tag{4}$$

where n is the dimensionality and (S/V_p) is the surface-to-pore volume ratio. The calculation is a perturbation expansion in the short time limit, closely related to the asymptotic expansion of the spectral function at short times [17] (see Section 2 for discussion), which relates geometrical quantities such as volume and surface to the Laplacian spectrum. The result by Mitra et al. is included in the Padé approximation, where A in Eq. 3 equals

$$A = \frac{4\sqrt{D_0}}{3n\sqrt{\pi}}(S/V_p). \tag{5}$$

The θ-parameter in the Padé approximation has the dimension of time and describes the rate of relaxation between the short and long time limits. $\sqrt{D_0\theta}$ expresses a characteristic length, the Padé length, related to the rate of relaxation. The Padé length is, in turn, expected to depend on the pore geometry [6,13] and some indications supporting this have been reported [6]. In this paper we connect standard spectral analysis of the diffusion operator with the parameters in Latour's approximation.

The time evolution of the probability density in a diffusion process is given by the partial differential equation

$$\frac{\partial \rho(\mathbf{r},t)}{\partial t} = D\Delta\rho(\mathbf{r},t), \tag{6}$$

with Neumann boundary conditions

$$\nabla \cdot \mathbf{n}\rho(S,t) = 0, \tag{7}$$

defining no flux of probability density through structure surface S where $\mathbf{n}$ is the outward pointing normal to the surface. A natural approach of solving this problem is to identify basis functions where the time and space dependence is separated $\rho_i(\mathbf{r},t) = f_i(\mathbf{r})g_i(t)$, and then express the full solution in this basis $\rho(\mathbf{r},t) = \sum_i \alpha_i \rho_i(\mathbf{r},t)$. This results in two separate eigenproblems in time and space, connected through shared eigenvalues. The eigenproblem in time, $\partial_t g_i = \lambda_i' g_i$, has exponential functions as solutions. The spatial eigenproblem is defined by the Helmholtz equation

$$\Delta f_i(\mathbf{r}) = -\lambda_i f_i(\mathbf{r}), \tag{8}$$

where λ_i equals

$$\lambda_i = \frac{\lambda_i'}{D_0}, \tag{9}$$

where λ_i' is the separative constant. A total solution to the diffusion equation is finally found as a linear combination of eigenvalue solutions, where the weights are chosen to match the initial conditions.

Finding analytical solutions to the spatial eigenvalue equations is in general not possible. The difficulty lies in imposing the Neumann conditions defined over complex geometries that describe the walls of the pores and the connecting channels. A special case when the eigenvalues can be found analytically is orthogonal bounding geometries (e.g. planar, cylindrical and spherical), including the extreme case of no boundary. In this case the general solution can be expressed in terms of harmonic eigenfunctions:

$$\rho(\mathbf{r},t) = \sum_{n=1}^{\infty} C_n e^{-t\lambda_n'} e^{2\pi i \mathbf{k}_n \cdot \mathbf{r}}. \tag{10}$$

To find numerical solutions to the diffusion equation, the Laplacian can be approximated by a discrete finite dimensional matrix

$$Lf(\mathbf{X}) = \lambda f(\mathbf{X}), \tag{11}$$

where we use a discrete approximation $L = -\Delta$ and $\mathbf{r} \to \mathbf{X}$, a discrete space vector. The numerical value of the elements of L depend on how we choose to discretize space. A simple, but often not optimal, choice is to use a regular grid. For a regular grid in d dimensions, the elements of L are defined as $L_{ii} = 2d\epsilon$ and $L_{ij} = -\epsilon$ if the nodes i and j are adjacent, where ϵ is defined by the spacing between nodes and can be interpreted as the probability of a particle to move from one node to an adjacent node.[1] This choice of discretization is often referred to as the finite difference method. In general, L is positive semi-definite. This follows from two properties of the Laplacian; integration by parts: (symmetry) $-\int_V dx f(x)\Delta g(x) = -\int_V dx g(x)\Delta f(x) + S$; and (positive semi-definite) $-\int_V dx f(x)\Delta f(x) = \int_V dx |\nabla f(x)|^2 + S$, where S is a surface term that vanish due to the Neumann boundary condition. It follows that L is diagonalizable and has real non-negative eigenvalues.

The total discrete solution of the diffusion equation is

$$\rho(t,\mathbf{X}) = \sum_{n=1}^{N} C_n e^{-t\lambda_n'} f_n(\mathbf{X}), \tag{12}$$

where f_n are eigenvectors to the Laplacian, L. In the special case of free diffusion, all eigenvectors f_n of L are discretizations of harmonic functions

$$v_n = e^{i\mathbf{k}_n \cdot \mathbf{X}}. \tag{13}$$

The wave vector $\mathbf{k}_n$, is written as [2]

$$\mathbf{k}_n = \frac{n_x 2\pi}{l_x}\hat{x} + \frac{n_y 2\pi}{l_y}\hat{y} + \frac{n_z 2\pi}{l_z}\hat{z}, \tag{14}$$

where n_x, n_y, n_z are the wave numbers and l_x, l_y, l_z are the lengths of the sample. In such a situation, the eigenvalues λ_n of L are

$$\lambda_n = |\mathbf{k}_n|^2 \tag{15}$$

and together with Eq. 9 we write the useful relation for the free diffusion constant

$$D_0 = \frac{\lambda_n'}{|\mathbf{k}_n|^2}. \tag{16}$$

The harmonic eigenfunctions appearing in the solution to free diffusion is used in Section 3 to calculate the tortuosity, by the ansatz of a harmonic solution in the long time limit. Before turning our attention to the tortuosity, a known spectral result regarding the relation between the Laplacian spectrum and the surface area and volume of void space is summarized and connected to the short time scale of $D(t)$.

2. Surface to volume ratio

The short-time expansion of the time-dependent diffusion coefficient by Mitra et al. [14,15] (Eq. 4) includes the surface-to-volume ratio of the void space as a proportionality factor. Formally, the void space is a domain to the Laplacian with Neumann boundary conditions. Extracting geometrical information of a domain from the Laplacian spectrum has been of large interest in the last century. In 1912 Weyl [18] proved a relation between the volume V, of the domain and the eigenvalues of the Laplacian. If $N(\lambda)$ denotes the number of eigenvalues smaller than λ, Weyl proved that

[1] L can also be interpreted as a generator of a Markov chain that describe a random walk between the nodes in the grid, see for example *Reversible Markov Chains and Random Walks on Graphs* by D. Aldous and J. Fill (http://stat-www.berkeley.edu/users/aldous/RWG/book.html) for details.

[2] The cumbersome indexing of the eigenvalues as n_{n_x,n_y,n_z} is not used but kept in mind.

$$N(\lambda) \sim \frac{V}{\left(\frac{d}{2}\right)!(4\pi)^{d/2}}\lambda^{d/2} \text{ as } \lambda \to \infty. \tag{17}$$

Hence it is possible to retrieve the volume of void space by studying the Laplacian spectrum. In order to obtain more detailed information certain functions of the spectrum are used. One such function is the trace function $T(t)$, representing the Laplace transform of $N(\lambda)$ [17]. The trace function thus equals

$$T(t) = \sum_n^{\infty} e^{-\lambda_n' t}, \tag{18}$$

which we note is the sum of the time functions to the solution of the diffusion equation. The three dimensional case still contain many open problems, so we restrict ourself in this very short review to the two-dimensional case where the corresponding surface-to-volume ratio is the perimeter-to-area ratio. We denote the pore surface area by A_p and the perimeter by P and we wish to obtain the quotient P/A_p. For a domain bounded by a broken line, for example the domain to a mesh Laplacian, Kac [19] (also [20]) proved that the trace function equals

$$T(t) = \frac{A}{4\pi t} + \frac{P}{4(4\pi t)^{1/2}} + \sum_{\text{corners}} \frac{\pi^2 - \alpha^2}{24\pi\alpha} + o(1) \text{ as } t \to 0 \tag{19}$$

where α is the inside-facing angle at the corner. Work by Kac [19], Pleijel [21], Gottlieb [22] show that if the resolution of the Laplacian is increased to the limit of infinite resolution, Eq. 19 transforms to

$$T(t) = \frac{A}{4\pi t} + \frac{P}{4(4\pi t)^{1/2}} + \frac{1-h}{6} + o(1) \text{ as } t \to 0 \tag{20}$$

where the last extra term denote the number of holes, h, in the domain. Many open questions remain regarding the connection between the trace function and the density function, but a recent result treats the above result in terms of the density function [23]

$$N(\lambda) = \frac{A}{4\pi}\lambda \pm \frac{P}{\pi}\sqrt{\lambda} + \frac{1-h}{6} \text{ as } \lambda \to \infty. \tag{21}$$

The last equation shows a direct relation between the area and perimeter of the void space and the Laplacian spectrum. Eq. 19 shows a disadvantage of using a rough mesh Laplacian, as the number of corners is not derivable from the spectrum. It may however be noted that the corner term is constant and the P/A_p-ratio may still be obtained by calculating several large eigenvalues of L and estimating the resulting slope. Interestingly the short-time expansion of Mitra et al. is similar to the above expressions and imply a direct relation to the Laplacian spectrum. However, as calculating the surface-to-volume ratio of void space via the Laplacian spectrum is a numerically intractable method, we stop here and conclude that the *largest eigenvalues of the Laplacian spectrum* relate to the surface-to-volume ratio of void space.

3. Tortuosity

In this section we discuss how the tortuosity parameter in Latourś approximation can be calculated using the spectrum of the Laplacian operator. The central idea is to use the ansatz that the solution to the diffusion equation has a Gaussian propagator in the long time limit, which is valid provided that the materials are spatially non-perfect. Similar approaches has been used earlier [24,2,14,16].

The general solution of the diffusion equation (Eq. 12) shows an exponential decay in time of all spatial eigenfunctions except those corresponding to zero eigenvalue (which is unique if the volume is connected, and represents the infinite time limit where the distribution is uniform). As a result, only the eigenvectors corresponding to the smallest eigenvalues of L contribute to the solution in the long time limit. Let the eigenvalues of L be ordered as

$$0 = \lambda_1 \leqslant \lambda_2 \leqslant \ldots \leqslant \lambda_N. \tag{22}$$

If the propagator is Gaussian in the long time regime, the eigenvectors corresponding to the first eigenvalues will be approximately harmonic. In fact the Gaussian approximation is valid, not only for the first smallest eigenvalues, but for all eigenvalues that have approximately harmonic eigenvectors with wavelength much longer than the typical size of the pores. Fig. 1 is an example of a porous system (inspired by chamber-and-throat networks [3]). The first eigenvectors of the associated Laplacian L are approximately harmonic implying that the corresponding propagator is approximately Gaussian. In the intermediate regime, the harmonic behavior is broken, meaning that the propagator is non-Gaussian. In Fig. 2 the first three eigenvectors to the Laplacian corresponding to the porous system in Fig. 1 have been extracted in the directions marked in Fig. 1 and shows a clear harmonic behavior.

The Gaussian behavior in the long time regime implies the following natural ansatz

$$Lv_n = \lambda_n v_n, \tag{23}$$

which is valid provided that n is small. v_n is the harmonic solution from Eq. (13) and λ_n is an eigenvalue to L. Using Eq. (16) we may now express the long time effective diffusion constant as

$$D_\infty = \frac{\lambda'}{|\mathbf{k}_n|^2}, \tag{24}$$

and calculate the tortuosity as

$$\tau_s^{-1} = \frac{D_\infty}{D_0} = \frac{\lambda_n}{k_x^2 + k_y^2 + k_z^2}. \tag{25}$$

The k_x, k_y and k_z can either be retrieved by solving Eq. (23) for a harmonic function of *known*, chosen wave numbers, or, by using the actual eigenfunctions, f_n, to the Laplacian and calculate the approximate wave numbers by a Fourier transform in the x, y and z-directions. The result is the tortuosity (with index s for "spectral") in direction

$$k_x\hat{x} + k_y\hat{y} + k_z\hat{z}. \tag{26}$$

If the structure is isotropic, the contribution is the same regardless of direction. For anisotropic structures the tortuosity will be different in different directions and several eigenvectors must be used in Eq. (25) to calculate the full diffusion tensor.

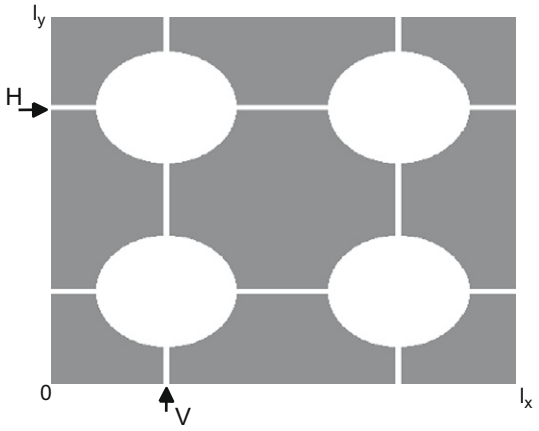

Fig. 1. A simple porous system. Each eigenvector was projected at the marked locations H (horizontal) and V (vertical) and are shown in Fig. 2.

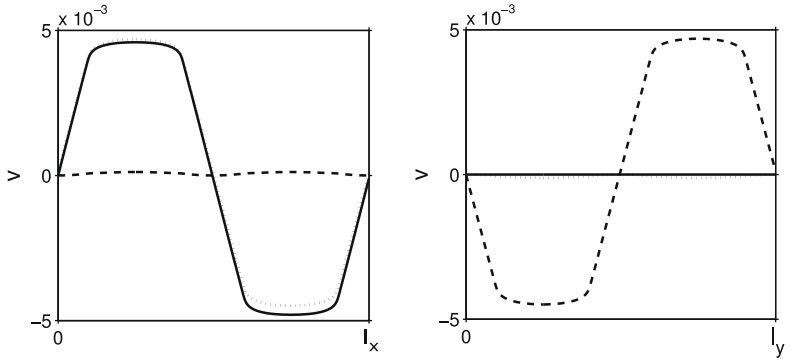

Fig. 2. The figure shows horizontal and vertical projections of the first three non-trivial eigenvectors of the Laplacian L of the porous system in Fig. 1 between 0 and l_x and 0 and l_y. The eigenvectors v_2 (dashed line), v_3 (dotted line) and v_4 (solid line) are projected in horizontal direction (left) and vertical direction (right) at the locations marked in Fig. 1. The eigenvectors are harmonic, implying a Gaussian behavior of the propagator.

4. Relaxation rate

In this section the relaxation rate of a diffusing particle in a porous system is estimated via the Laplacian spectrum. We assume here that the material consists of pores with narrow connections. This results in a natural time-scale separation between the two processes where particles diffuse within the pores and where particles diffuse in a pore-to-pore mode. As the time evolution of the propagator is closely related to the Laplacian spectrum, the time-scale separation is identified as a discontinuity in the spectral density, a *spectral gap*.[3] We then use the ansatz that the time-dependent diffusion coefficient is of the same form as the Padé expression, with a relaxation parameter connected to the spectral gap. As mentioned in the previous section, if the propagator is approximately Gaussian in the long time limit the diffusion equation is valid, not only in the short time limit where the time-dependent diffusion coefficient equals the unrestricted diffusion constant D_0, but also approximately for long times where $D(t)$ converges to D_∞. We question at *what rate* the time-dependent diffusion coefficient $D(t)$ converges from the unrestricted diffusion with D_0 towards the pore-to-pore mode with D_∞? From the time evolution of the diffusive behavior in a porous system (Eq. (12)), it can be noted that the amplitude of each eigenvector v_n, will decay with $e^{-t\lambda_n}$. The contribution for v_n, therefore is time-dependent and is determined by the magnitude of the eigenvalue λ_n. The eigenvalues of L thus represent different time scales for the diffusive behavior in the porous system given. We call the first large shift in the eigenvalue spectrum of L a spectral gap. For a system with a wide pore size distribution the spectral gap is less pronounced, as the point in time for when particles begin to move in a pore-to-pore mode is dependent on the probability for a particle to exit its pore. Fig. 3 shows an example of a porous system with a pore size distribution and Fig. 4 shows the corresponding Laplacian spectrum 1 together with the Laplacian spectrum of the pore system in Fig. 3 as a reference.

The spectral gap can be used to define the transition rate between the short and long time diffusive behavior in the system. Starting with a probability distribution described by all eigenmodes to L most of the eigenmodes describe diffusion within pores. Let $\lambda_\uparrow$ be the eigenvalue corresponding to the slowest relaxing eigenmode of the eigenmodes that describe diffusion *within* pores and let $\lambda_\downarrow$ be the eigenvalue corresponding to the fastest eigenmode representing diffusion in a pore-to-pore mode. These eigenvalues are precisely the eigenvalues at each side of the spectral gap (see Fig. 4). If we approximate the system to be described by these two states, we question at what rate the system transfer from diffusion within pores to the pore-to-pore diffusive mode? This two-state approximation of the system can be written as

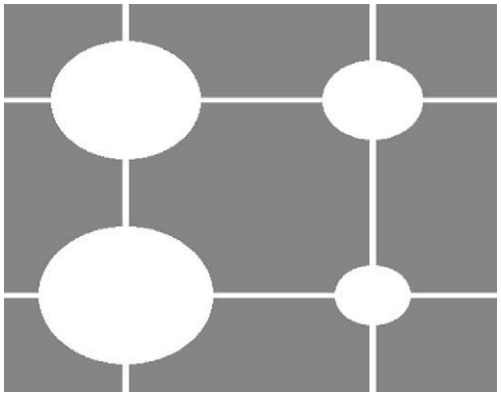

Fig. 3. A simple porous system with different pore sizes.

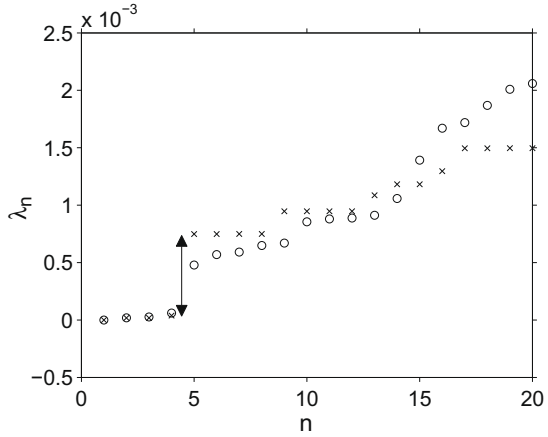

Fig. 4. The first 20 eigenvalues of two Laplacians corresponding to the porous system with a fixed pore size (Fig. 1) (×) and similar system but with a pore size distribution (Fig. 3) (o). The spectral gap, marked with an arrow for the system with fixed pore sizes, is made less distinct by broadening the pore size distribution as the pore-to-pore mode is reached in a time that depends on the pore size. Hence the time for the pore-to-pore mode is "smeared out" with a broader pore size distribution.

[3] A common definition of the spectral gap is the first non-trivial eigenvalue, but in this paper, the spectral gap is defined as *the first significant gap* in the spectrum. In the extreme case when the pores are completely disconnected the two definitions are equivalent but our definition is more useful when the pores are connected through narrow channels.

$$\rho(\mathbf{r}(t),t) = C_\uparrow e^{-\lambda'_\uparrow t} f_\uparrow + C_\downarrow e^{-\lambda'_\downarrow t} f_\downarrow. \quad (27)$$

We introduce a threshold C_{thr} for when the system is considered to be dominated by $\lambda_\downarrow$

$$C_{thr} = e^{-t(\lambda'_\uparrow - \lambda'_\downarrow)}, \quad (28)$$

This gives a time θ_s, when the system is considered to be dominated by the pore-to-pore mode as

$$\theta_s = \frac{\log(C_{thr})}{D_0(\lambda_\uparrow - \lambda_\downarrow)}. \quad (29)$$

We now use the following ansatz

$$\frac{D(t)}{D_0} = 1 - (1-\tau_s^{-1}) \times \frac{A\sqrt{t} + (1-\tau_s^{-1})\theta_s^{-1} t}{(1-\tau_s^{-1}) + A\sqrt{t} + (1-\tau_s^{-1})t\theta_s^{-1}}, \quad (30)$$

an expression equivalent with the Padé approximation (note the subscript s for both the tortuosity and relaxation parameter indicates that the quantity is derived through spectral analysis). The tortuosity τ_s is calculated in Eq. (25) and $A = 4\sqrt{D_0}/9\sqrt{\pi}(S/V_p)$, the expression worked out by Mitra et al. [14] (higher order terms are neglected). Eq. (30) is of the same form as the Padé expression (see Eq. (3)) and the parameter τ can be identified as τ_s (see Eq. (25)) and the relaxation parameter θ as θ_s. The relaxation parameter θ_s, works here as a bridge between the short-time (free or non-obstructed) diffusion equation with $D(t)/D_0 = 1$, and the long time pore-to-pore diffusion equation with $D(t)/D_0 = \tau_s^{-1}$. As θ_s is the time where the system is considered to be in the long time pore-to-pore mode, this gives an interpretation of the Padé parameter, θ, for systems with a clear spectral gap. For such systems, the characteristic Padé length $\sqrt{D_0\theta}$ is proportional to

$$\sqrt{D_0\theta} \propto (\lambda_\uparrow - \lambda_\downarrow)^{-1/2}. \quad (31)$$

Hence, the geometrical impact on the Padé length can be captured by the gap in the spectrum of L.

5. Calculations

In our calculations we created porous systems with periodic boundary conditions. The periodic boundary conditions avoid artefacts related to closure of a finite volume, e.g. in a closed box there is no well-defined diffusion at longer time scales. Explicit particle simulations, used to compare the results from the spectral analysis, where performed using a particle that jumped a distance chosen from a Gaussian probability distribution during one time step. If the jump was too large, as defined by a cutoff radius, or a collision with the boundary occurred, the jump was subdivided into several smaller jumps until a valid trajectory had been calculated. A typical simulation used 50,000 particles and 400,000 time steps and took about 8 h to perform on a standard PC.

The discretization of space was performed by applying a regular grid on the porous system, with minimum connectivity, meaning that each pixel has at most four neighboring pixels. Each pixel may then be mapped to entries in a matrix A such that $A_{i,j} = 1$ if pixel i and j are connected. The Laplacian matrix may then be expressed as $\epsilon^{-1}L = \mathrm{diag}(\sum_i A_{i,j}) - A$ (to be compared with the Laplacian matrix introduced in Section 1). The eigenvalues/eigenvectors can now be directly calculated by diagonalizing the large but sparse matrix L. The diagonalization was performed with LAPACK routines in MATLAB and 20–30 eigenvalues/eigenvectors could be extracted within 0–3 h depending on the size of L. To extract the wave numbers (Eq. 25) the eigenvectors of L are mapped back to the geometry and a (FFT) Fourier transform, may be performed in each orthogonal direction. The structure itself imposes frequencies which have to be filtered out, in example by Fourier transforming the trivial eigenvector however, the wave length of the lowest eigenvectors is directly seen by plotting the eigenvectors. With the **k** vectors Eq. (25) may be used for deriving the tortuosity, which is valid provided that the wavelength of the **k** is larger than the length scale of the micro structure, or in other words that the eigenvalue is sufficiently small for the corresponding eigenvector to have a clear frequency. The spectral gap is obtained by plotting the spectrum of eigenvalues, for this, sufficiently many eigenvalues must be extracted.

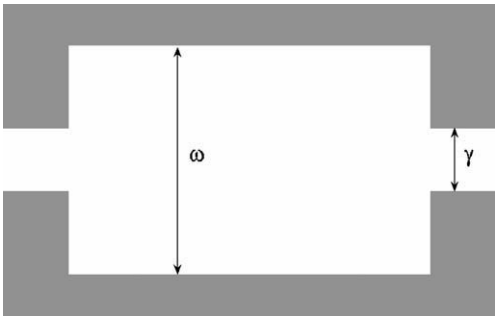

Fig. 5. A pore cell. The pore width ω was varied from $\omega = \gamma$ to $\omega = 4\gamma$.

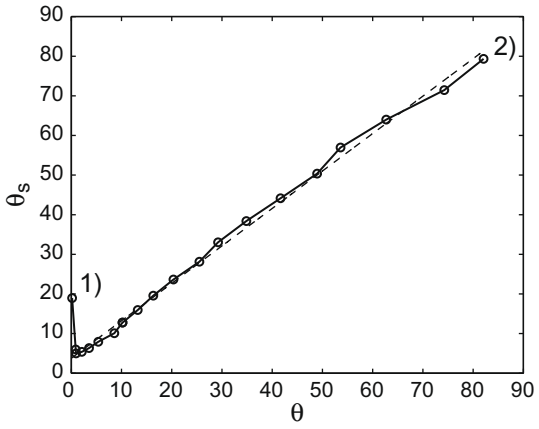

Fig. 6. The pore width ω of the porous system in Fig. 5 was varied and for each ω simulations and calculations where carried out. The figure shows comparson of θ_s calculated from the Laplacian spectrum versus the relaxation rate θ retrieved by fitting the Padé approximation to simulations. (1) $\omega = \gamma$. (2) $\omega = 4\gamma$. The dashed line is a linear fit.

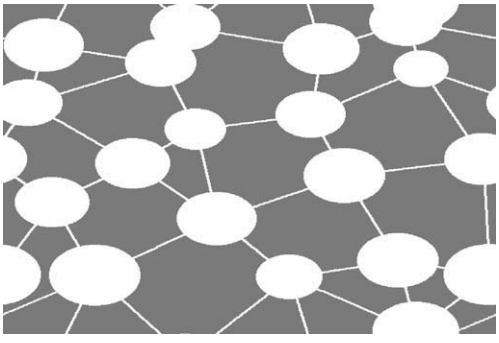

Fig. 7. A porous system consisting of connected pores of different sizes at random locations. The material in the picture represents a random pore structure on the length scale defined by the box. At longer length scales the material is clearly not random due to the periodic boundary conditions. This artifact does however not affect the eigenvalues and eigenvectors corresponding to wave numbers contained within the box.

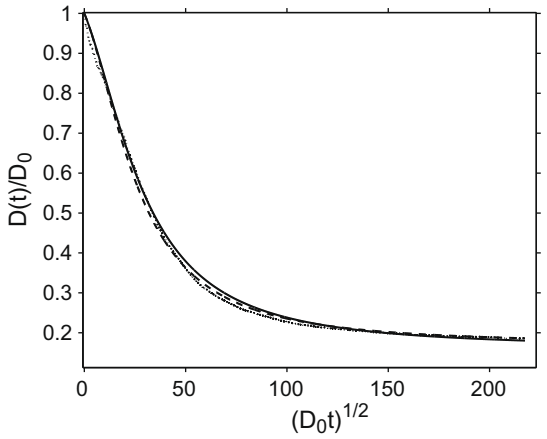

Fig. 8. Comparson of simulation (dotted line), best Padé fit (dashed line) and expression 30 (solid line) of the porous system in Fig. 7.

Table 1
Data for all structures presented. The diffusion constant D_0 equals 1 [pixels^2/s].

Structure	τ_s^{-1}	$D(\infty)/D_0$	θ_s [s]	θ [s]
Fig. 1	0.172	0.165	1376.2	1305.0
Fig. 3	0.182	0.181	2339.2	1811.6
Fig. 5 ($\omega = 4\gamma$)	0.091	0.085	79.1	82.7
Fig. 7	0.181	0.180	1196.2	1063.8

6. Simulation and discussion

To test the validity of Eq. (30) explicit Brownian motion simulations described in the previous section where carried out in various porous systems. The simulation time was taken to give a diffusive length of at least 10 times the unit cell length and $40k - 120k$ particles where used depending on the amount needed for the mean square displacement to converge. The simulation outcome $D(t)/D_0$ was plotted against time and the long time effective diffusion constant $D(\infty)/D_0$ was estimated. The Padé approximation [6] (Eq. (3)) was fitted to the simulation data and from that the relaxation parameter θ was estimated. $D(\infty)/D_0$ and the θ-parameter where compared with θ_s calculated from Eq. (29) (where a threshold of 1% was used, note that due to the log function θ_s is relatively insensitive to the numerical value of the threshold) and τ_s^{-1} calculated from Eq. (25). To retrieve the surface-to-volume ratio, a large resolution of the mesh Laplacian is needed. The surface-to-volume ratio was therefore not calculated but estimated from the initial slope of $D(t)/D_\infty$. First a single pore cell was used (see Fig. 5) where the pore width ω was varied from having the same width as the connector, γ, to being significantly larger. A comparison of θ_s and θ (Fig. 6) shows a clear linear dependence as the pore gets large relative to the connector. This shows that for systems with large pores and thin connectors, the spectral gap is a good estimate of the relaxation time. It is interesting to note that the Padé approximation is still valid in the situation where $\omega = \gamma$ and no clear spectral gap is present. A more complicated structure is presented in Fig. 7 where a pore distribution has been used at random locations resulting in varying lengths for the connections. Fig. 8 shows expression 30 together with simulation data and the best Padé fit of simulation data. The surface-to-volume ratio was estimated from the simulation data. In this case several characteristic diffusive lengths are present, which results in a spectral gap with several intermediate states. The relaxation rate estimated from the spectrum is however still in good agreement with the simulation. The long time effective diffusion constant estimated from the spectrum (Eq. (25)) is, as expected, also in accurate agreement with the results from the explicit simulations. Table 1 shows calculated parameters, the estimated relaxation rate from the fitted Padé expression and the long time behavior $D(\infty)/D_0$ estimated from the simulation outcome for all structures presented.

7. Conclusions

In this paper we have shown that it is natural to describe diffusion in porous materials in terms of the Laplacian spectrum (see Fig. 9 for a schematic view). The three parameters τ, (S/V_p) and θ in the Padé approximation suggested by Latour et al. [6], can all be explained by details in the Laplacian spectrum. Computationally, the Laplacian of a porous system is approximated by a matrix L, that includes the Neumann boundary conditions defining no flux through the surface of the pore structure. The tortuosity, τ, is retrieved by calculating the smallest eigenvalues of L. This approach is general and works not only for porous systems, but for all systems where a long time effective diffusion constant exists. The sur-

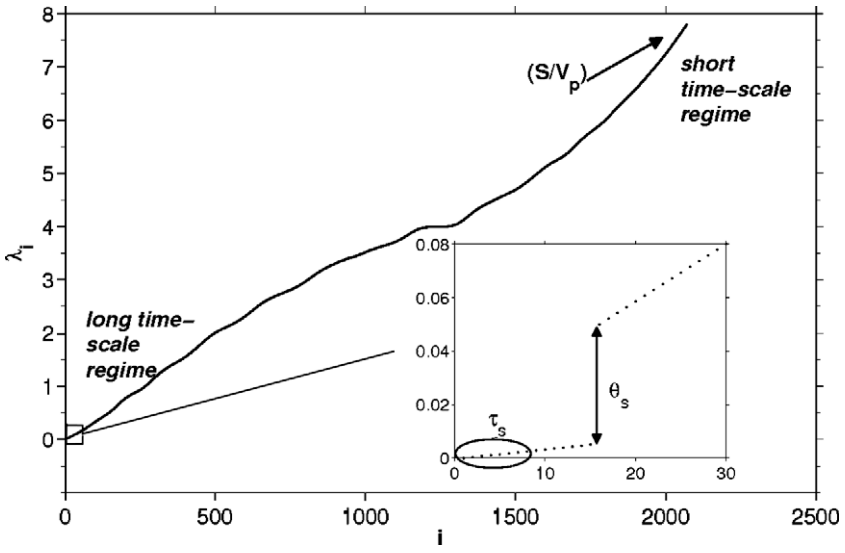

Fig. 9. Schematic view over Laplacian spectrum and diffusion parameters.

face-to-volume ratio, (S/V_p), is estimated from the slope of the spectrum at large eigenvalues. For porous systems with a large pore-to-connector length ratio, the spectral gap can be used as a good approximation of the relaxation rate. It turns out that the Padé length, $\sqrt{D_0\theta}$, for such systems directly relates to the geometry, via the spectral gap in the Laplacian spectrum. However, the Padé approximation seem to work well also for some systems that does not inhibit a clear time-scale separation (see also for example [13]). The rate of relaxation is in these cases not directly obtained from the spectral gap approach presented here. At present the full relationship between the relaxation parameter in the Padé approximation and the Laplacian spectrum is not known, but the fractional form of the Padé approximation works as a good interpolation for the time-dependent diffusion coefficient. In general it is however clear that the full relaxation process can in principle be found by a complete eigenfunction expansion of the Laplacian.

To summarize; Large eigenvalues of the Laplacian describe $D(t)$ at short times, and spectral analysis connects the surface and volume to the large eigenvalues of the Laplacian. The ratio (S/V_p), can be estimated from the slope of large eigenvalues of the Laplacian. The long time effective diffusion constant can be derived via small non-trivial eigenvalues of the Laplacian. For systems with a clear pore structure, the rate of relaxation, θ_s, can be computed from the spectral gap of the Laplacian spectrum. A spectral gap in the spectrum implies a clear time-, and thereby also length-, scale separation in the system. One such example is a system with a large pore-to-connector volume ratio.

References

[1] P.T. Callaghan, A. Coy, D. MacGowan, K.J. Packer, F.O. Zelaya, Diffraction-like effects in nmr diffusion studies of fluids in porous solids, Nature 351 (6326) (1991) 467–469.

[2] P.T. Callaghan, Principles of Nuclear Magnetic Resonance Microscopy, Oxford University Press, 1991.

[3] V.N. Burganos, A.C. Payatakes, Knudsen diffusion in random and correlated networks of constricted pores, Chem. Eng. Sci. 47 (6) (1992) 1383–1400.

[4] L.L. Latour, R.L. Kleinberg, P.P. Mitra, C.H. Sotak, Pore-size distributions and tortuosity in heterogeneous porous media, J. Magn. Reson. Ser. A 112 (1) (1995) 83–91.

[5] J. Qian, P.N. Sen, Time dependent diffusion in a disordered medium with partially absorbing walls: a perturbative approach, J. Chem. Phys. 125 (19) (2006) 194508.

[6] L.L. Latour, P.P. Mitra, R.L. Kleinberg, C.H. Sotak, Time-dependent diffusion coefficient of fluids in porous media as a probe of surface-to-volume ratio, J. Magn. Reson. 101 (3) (1993) 342–346.

[7] S. Olayinka, M.A. Ioannidis, Time-dependent diffusion and surface-enhanced relaxation in stochastic replicas of porous rock, Trans. Porous Media 54 (2004) 273–295.

[8] M. Regier, H.P. Schuchmann, Monte carlo simulations of observation time-dependent self-diffusion in porous media models, Trans. Porous Media 59 (2005) 115–126.

[9] M.D. Hürlimann, K.G. Helmer, L.L. Latour, C.H. Sotak, Restricted diffusion in sedimentary rocks. Determination of surface-area-to-volume ratio and surface relaxivity, J. Magn. Reson. Ser. A (1994).

[10] G.P. Frosch, J.E. Tillich, R. Haselmeier, M. Holz, E. Althaus, Probing the pore space of geothermal reservoir sandstones by nuclear magnetic resonance, Geothermics 29 (6) (2000) 671–687.

[11] R.W. Mair, M.D. Hürlimann, P.N. Sen, L.M. Schwartz, S. Patz, R.L. Walsworth, Tortuosity measurement and the effects of finite pulse widths on xenon gas diffusion nmr studies of porous media, Magn. Reson. Imaging 19 (2001) 345.

[12] R.W. Mair, P.N. Sen, M.D. Hürlimann, S. Patz, D.G. Cory, R.L. Walsworth, The narrow pulse approximation and long length scale determination in xenon gas diffusion nmr studies of model porous media, J. Magn. Reson. 156 (2002) 202.

[13] H. Pape, J.E. Tillich, M. Holz, Pore geometry of sandstone derived from pulsed field gradient NMR, J. Appl. Geophys. 58 (3) (2006) 232–252.

[14] P.P. Mitra, P.N. Sen, L.M. Schwartz, P. Le Doussal, Diffusion propagator as a probe of the structure of porous media, Phys. Rev. Lett. 68 (24) (1992) 3555–3558.

[15] P.P. Mitra, P.N. Sen, L.M. Schwartz, Short-time behavior of the diffusion coefficient as a geometrical probe of porous media, Phys. Rev. B 47 (14) (1993) 8565–8574.

[16] K. Dunn, D. Bergman, Self diffusion of nuclear spins in a porous medium with a periodic microstructure, J. Chem. Phys. 102 (8) (1995) 3041–3054.

[17] B.D. Sleeman, E.M.E. Zayed, Trace formulae for the eigenvalues of the Laplacian, J. Appl. Math. Phys. 35 (1984) 106–115.

[18] H. Weyl, Das asymptotische verteilungsgesetz der eigenwerte linearer partieller differentialgleichungen, Math. Ann. 71 (1912) 441–479.

[19] M. Kac, Can one hear the shape of a drum?, Am Math. Mon. 73 (1966) 123.

[20] H.P. McKean Jr., I.M. Singer, Curvature and the eigenvalues of the Laplacian, J. Differ. Geometry 1 (1967) 43–69.

[21] Å ke Pleijel, A study of certain green's functions with applications in the theory of vibrating membranes, Arkiv fr Matematik 2 (1954) 553–569.

[22] H.P.W. Gottlieb, Eigenvalues of the Laplacian with Neumann boundary conditions, Austral. Math. Soc. Ser. B 26 (1985) 293–309.

[23] W. Dai, M. Xie, The number of eigenstates: counting function and heat kernel, J. High Energy Phys. 2009 (2009) 1–16.

[24] E.O. Stejskal, J.E. Tanner, Spin diffusion measurements: spin echoes in the presence of a time-dependent field gradient, J. Chem. Phys. 42 (1) (1965) 288–292.